

Traumatic Brain Injury Investigation Using FE Modeling of the Rat and Experimental High Amplitude Rotations in the Sagittal Plane

M. Lamy , D. Baumgartner , J. Davidsson and R. Willinger

Abstract A combined approach of numerical modeling and animal experiments was used to study the mechanisms of traumatic brain injury (TBI). A three-dimensional finite element model (FEM) of the rat brain was submitted to experimental sagittal plane rotational acceleration pulses. The experimental setup provided histological analysis of injured brain tissues for a range of severities. The biomechanical response parameters were extracted from the FEM in the anatomical regions identified by experiments as prone to injuries. Von Mises stresses and first principal strains proved to increase with both the amplitude of acceleration loadings and the tissue injuries severities. Further comparison between mechanical responses and experimental histological scores allowed proposing tissue thresholds for the occurrence of TBI, namely 1.5 kPa and 4% approximately for Von Mises stresses and first principal strains, respectively. Those values can be used for further investigations of the mechanisms of TBI.

Keywords animal experiments, finite element modeling, injury mechanisms, traumatic brain injury

I. INTRODUCTION

In modern society, Traumatic Brain Injuries (TBI) represent a major health issue. Depending on their intensities, they can generate many consequences. While cases considered as being mild can result in temporary impairments, the most severe cases can eventually be responsible for lifelong disabilities or even death. In Europe, it has been estimated that TBI affect 235 out of 100,000 persons every year [1]. In the United States, it has been reported that approximately 1,700,000 cases of TBI occur per year [2]. Falls represent the main cause of TBI, followed by traffic incidents and sports-related activities, though traffic incidents are the first cause in terms of mortality rate. Populations most at risk of sustaining TBI are young children under 4 years, adolescents and young adults (16 to 24 years), and adults aged 65 years or older. Furthermore, TBI are not only a health issue but also affect a country's economics. In addition to obvious costs in terms of health treatments (approximately \$76.5 billion in 2010 in the US [2]), they also have a long-term financial impact, as victims of TBI-induced severe disabilities might no longer be able to be productive. As a consequence, over the past years, many projects have focused on reducing the severe outcomes and mortality rate of TBI, for example through the development and improvement of protective systems in automotive environments or of protective equipment in sports. However, if better protection or even prevention of TBI is to be achieved, it is of utmost importance to constantly improve further the state of understanding of the biomechanics of head injuries.

It has been postulated that the complex loading conditions of collision forces are correlated with the mechanisms leading to the occurrence of TBI. In particular, a major focus has been placed on head acceleration [3]. In real life, whatever the global complexity of a collision, its acceleration parameter can be separated into two distinct components, linear and rotational, both of which have potential direct consequences for injuries. The linear component has been studied and depicted to be generally responsible for focal brain injuries, and it has also been correlated to intracranial pressure changes [4]. Linear acceleration has often been used as a component for criteria and indexes that are used in standards or validation procedures. One such index is the Head Injury Criterion (HIC) which is based on the linear acceleration of the head and is widely used in the automotive industry for designing protective structures. However, the HIC has generated some controversies

M. Lamy is Post Doctoral Student in Applied Biomechanics at Polytechnique Montréal - Canada. D. Baumgartner is Asst Prof in Biomechanics at the University of Strasbourg, France (tel: +33 3 68 85 29 42, daniel.baumgartner@unistra.fr). J. Davidsson is Project Manager at the Division of Vehicle Safety at Chalmers University of Technology, Sweden. R. Willinger is Prof in Biomechanics at the University of Strasbourg, France.

over the years [5], in particular for taking into account only one part of the global acceleration parameter. Indeed, the angular component of acceleration, while oft-ignored by many criteria, has also long been established as an important factor in brain injury occurrences and mechanisms [6]. It has even been reported to be the main contributor to TBI, more than the linear component [7-8]. Nevertheless, it very rarely is taken into account for the validation of protective systems [9].

In this regard, TBI and the complex collision conditions under which they are alleged to occur are important research areas. But, as information about human TBI can only be obtained a posteriori, works in these areas require animal and numerical models. On the experimental side, rodent, and especially rat, models have often been used for studying neurotrauma and documenting behavioral or physiological changes and deficits. Different types of models, and consequently of lesions, have been developed: controlled cortical impact [11-12], dynamic cortical deformation [13], fluid percussion [14-15], direct head impact weight-drop [16] and rotational accelerations [17-22]. Though several finite element models of the rat brain exist [22-27], to our knowledge no complete three-dimensional finite element model of a rat brain was used for the simulation of very high amplitude angular acceleration loadings in a sagittal plane. Yet, outcomes from TBI-specific experiments can be used as loadings for finite element models to determine the local responses of the rat brain. As such, the present computational study aimed to determine and analyze the intrinsic mechanical responses of the different anatomical regions of the brain in reaction to a rearward sagittal rotational acceleration collision.

Based on the foregoing observations and brief review, and the importance of region-specific responses, a finite element model of the rat head was submitted to experimental data to better understand the brain biomechanical behavior under angular acceleration loadings leading to TBI. Specifically, tissue responses were analyzed and compared to histological evidence to propose thresholds for the occurrence of TBI.

II. METHODS

Experimental Testing

An in vivo animal model that produces diffuse brain injury (DBI) in sagittal plane rearward rotational acceleration was used to produce injury data for this study. The model has been presented and the injuries characterized in the past [17-20]. In this model, the skull of anesthetized adult rats, Sprague-Dawley rats weighing 0.415 kg in average, was tightly secured to a rotating bar. During trauma, the bar was impacted by a striker that caused the bar and the animal head to rotate rearward; the acceleration phase lasted 0.4 ms and was followed by a rotation at constant speed and gentle deceleration when the bar made contact with a padded stop. The total head angle change was less than 30 degrees. By adjusting the air pressure in the rifle used to accelerate the striker, resulting rotation acceleration between 0.37 and 2.10 Mrad/s² were achieved. The work was performed in accordance with the Swedish National Guidelines for Animal Experiments which was approved by the Animal Care and Use Ethics Committee in Umeå.

For detection of axonal injuries, the animals were sacrificed 3 to 120 h post trauma, the brains removed and fresh frozen on dry ice. Coronal 14 μ m cryostat sections from three regions, front, middle and occipital, of the brains were cut and incubated with antibodies for beta-amyloid precursor protein (β -APP) for detection of axonal injuries. In situ hybridization was carried out with probes for cyclooxygenase 2 (COX-2). The latter is an enzyme responsible for formation of important biological mediators; it has been reported to be abundant in cells at sites of inflammation and has been suggested to correlate with cell death [19, 28-29].

In the histological analysis, brain sections from each of the three brain regions were chosen arbitrarily and antibody reactivity was assessed with a NIKON E600 microscope equipped with a confocal C1 unit or traditional white light according to a grading schema (Table 1).

TABLE 1
GRADING OF β -APP AND COX-2

Grade	Number of β -APP-positive axons per section	Shape and dimension of β -APP-positive axons	Intensity of COX-2 silver staining per section	Localization of the COX-2 positive cells
0	Only slight β -APP stains in cell body	–	Sometimes visible	Distributed regardless of tissue type
1	50 - 100	Small but asymmetric	Visible in 10 x microscope	Localized to cell bodies
2	100 - 200	Large and asymmetric	Visible in 1x microscope, bright contrast underlying tissue	Localized to cell bodies
3	> 200	Large and some extended along the axon	Visible macroscopically and overshadowing tissue behind	Localized to cell bodies

Finite Element Model Description

A three-dimensional finite element model of the rat head has been developed. Data for this model were obtained through medical imaging techniques used on a Sprague-Dawley rat. Magnetic Resonance Images displaying a voxel size of 500 μ m x 500 μ m x 500 μ m allowed for the acquisition of the soft cerebral tissue geometry. In both situations, geometrical data were extracted by realizing a segmentation of the medical images. The result was a surface triangular grid of the external brain surface which served to define the volume to be meshed to represent the brain in the model.

Commercial software (Altair HyperMesh 10.0[®] Troy MI, USA) was used to create the mesh defining the brain volume. Volume elements in the model were exclusively eight-node hexahedral elements, while four-node were all shell elements, with a standard Lagrange integration scheme. The average edge size for the elements was chosen as 0.45 mm. In addition to edge size, other criteria were defined, among which were the warpage of the faces of the finite elements, the aspect ratio of its edge sizes and the global skewness. They were based upon those which had been used for our Strasbourg University Finite Element Head Model (SUFEHM) [30]. Those criteria were strictly controlled during the whole meshing step so that the resulting mesh would be as regular as possible and that irregular elements, which would possibly degenerate during simulations, were avoided. The criteria are summarized in table 2.

TABLE 2
SUMMARY OF THE FEM CRITERIA

Criterion	Chosen value	Respect of criterion	Range	Supplementary information
<i>Minimum length</i>	> 0.45mm	100%	0.45mm - 0.68mm	0.45mm<Min length<0.55mm: 96.7%
<i>Maximum length</i>	< 1.5mm	100%	0.49mm - 1.5mm	0.49mm<Max length<1mm: 85,5%
<i>Warpage</i>	< 40°	100%	0° - 39.79°	Warpage<20°: 90.8%
<i>Aspect Ratio</i>	< 5	100%	1.06 - 3.18	Aspect ratio <2.5: 98.3%
<i>Skewness</i>	< 60°	100%	0.03° - 59.58°	Skewness<30°: 80.5%
<i>Jacobian</i>	> 0.7	90.7%	0.4 - 1	Jacobian>0.6: 95.4% Jacobian>0.5: 98.6%

The achieved finite element mesh of the brain volume consisted of 14,752 hexahedral elements. This brain was itself subdivided into 22 anatomical components. 18 of those 22 components represented internal

divisions of the cerebrum. The brain mesh is shown in Figure 1. Another component made of a single continuous layer of 3,220 hexahedral elements was created to encase the brain and represent both the cerebrospinal fluid and the meninges. Eventually, a layer of 3,220 shell elements (constant thickness of 0.1 mm) was added on the external surface of the model to represent the inner surface of the skull. This simplified skull was chosen because the skull only had to confine the brain. Furthermore, the skull component was defined as a rigid body and therefore the whole skull geometry was not needed. Thus, the complete FE mesh of the model consisted of 24 components which were continuous in themselves and between each other.

Following the initial meshing steps, material properties were assigned to the components of the model, once again through the use of commercial software (Altair Hypercrash 10.0[®], Troy MI, USA). Several assumptions were decided for the model. First, all the elements were considered as being homogeneous and isotropic. Then, brain elements were assumed to be made of gray matter. Literature was then explored for the soft tissue mechanical behaviors. Properties for the skull and for the brain/skull interface were based upon finite element modeling studies from our group as well as research from Wayne State University [26, 31]. The skull, in particular, received an elastic behavior with a Young modulus similar to the one used in the SUFEHM; though studies have shown that this elastic modulus could have lower values [32-33], the current model kept a 15 GPa value as it would not be used to simulate fracture occurrences. Also, the skull was defined as a rigid body for this work's simulations, lessening the skull's elastic modulus influence. The other components representing the brain were assigned a linear viscous elastic material behavior, defined by a Boltzman law [24, 26], with associated mechanical parameters based on the literature [22]. The choice of a linear viscous elasticity instead of other material models, such as hyperelastic or nonlinear viscous elastic ones, was made for practical reasons. Available data for those other models are quite scarce, even more so than for linear viscous elastic models, especially when considering rats specifically. The short-term shear modulus was chosen, in accordance with MRE data from our laboratory [34], to be appropriate for the very short duration loading which was to be simulated. The assumed homogeneity of brain matter was also partly dependent on this choice; regional mechanical properties can be found in the literature [35-38], but there are strong differences in modeling choices concerning the relative stiffnesses of grey and white matter [24, 26]. Also, those studies were not dealing with high-frequency loadings like the ones in this study. Consequently, homogeneity of brain matter with a short-term shear modulus suitable for the loading frequency was preferred to heterogeneity and uncertainty on this heterogeneity at high frequencies. Table 3 includes the material properties as well as detailed descriptions of the components used in the finite element model.

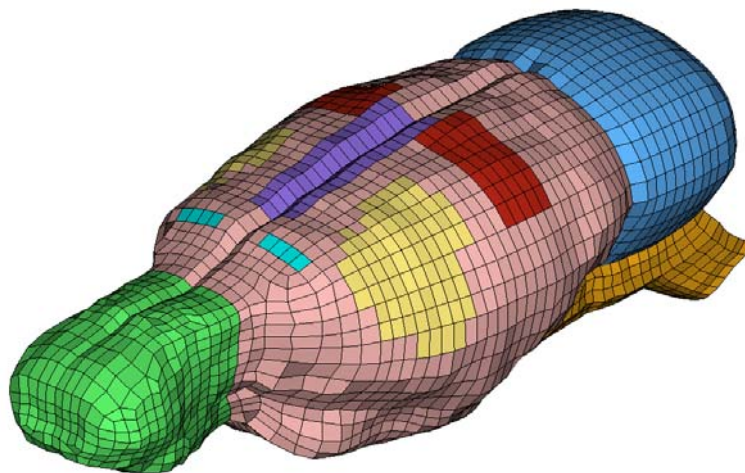


Figure 1. Display of the three-dimensional Finite Element Model of the rat brain which was used in the current study. The olfactory bulbs are present at the far left, while the cerebellum (upper) and the brainstem (lower) are at the far right on the picture. The central cortex exhibits some internal sub-components on the picture.

The cerebrospinal fluid and meninges layer as well as the skull are not displayed in the figure.

TABLE 3
MATERIAL PROPERTIES OF THE ANATOMICAL COMPONENTS OF THE MODEL
(Numbers of elements are indicated in parentheses)

Cerebrum (6,374), Cerebellum (2,634), Brainstem (1,484), Olfactory bulbs (1,390), Orbitofrontal cortex (420), Cingulate cortex (216), Parietal cortex (494), Striatum (366), Septum (30), Thalamus (198), Hypothalamus (152), Amygdala (24), Hippocampus (354), Temporal cortex (74), Ventral tegmental nuclei (14), Mesencephalic tegmentum (32), Occipital Cortex (254), Superior Colliculous (94), Entorhinal cortex (54), Aqueduct (24), Subiculum (46), Inferior Colliculous (24)	Density (kg/m ³)	1,040
	Short term shear modulus (kPa)	10
	Long term shear modulus (kPa)	2
	Bulk modulus (GPa)	2.19
	Decay constant (s ⁻¹)	0.125
Layer of hexahedral elements connecting the skull to the brain (Single continuous layer representing the meninges and cerebrospinal fluid - 3,220)	Density (kg/m ³)	1,130
	Young modulus (MPa)	20
	Poisson's ratio	0.45
Skull (3,220)	Density (kg/m ³)	1,800
	Young modulus (MPa)	15,000
	Poisson's ratio	0.21

Model Validation

The model efficiency was established by performing simulations of protocols of dynamic cortical deformation (DCD) based upon experimental data [23]. In these protocols and in our corresponding simulations, the left cortex, which had been exposed through a craniectomy, was submitted to vacuum pressure pulses of varying durations and amplitudes. The simulated displacements of the exposed brain surface were extracted before being compared to the experimental measures.

Results from the validation simulations were published in a previous IRCOBI study [39]. Simulated displacements were of the same order of magnitude as the experimental ones. The slightly lower values in simulations compared to experiments were considered to be due to the choices in the mechanical parameters. Those parameters were selected to be adapted for acceleration loadings of high amplitudes and short durations [22, 34], but may not have been as appropriate for the lower-frequency DCD protocols. Still, the results were deemed acceptable.

Numerical Simulations

The finite element model was submitted to different sagittal plane rearward rotational acceleration pulses. Each pulse was based upon experimental angular acceleration versus time data [17-20]. Eventually, 47 acceleration cases were available and each one of them served as a loading case for a specific numerical simulation. To do so, the acceleration loading data were applied directly to the rigid skull component. Figure 2 shows a representative plot of the typical rotational acceleration versus time history for the current study. The mean duration of the main acceleration peak in the different cases was approximately 0.4 ms. In terms of maximal amplitude of the angular acceleration, the loadings varied from 0.37 Mrad/s² to 2.10 Mrad/s². The simulations all shared the same material properties. The mechanical analysis was conducted with commercial software (Radioss Crash[®] solver, Altair HyperMesh 10.0[®] Troy MI, USA) on a standard personal computer with an Intel core 2 DUO[®] processor running at 3.33 GHz with 2 GB of RAM. As far as performances are concerned, simulations were run for 10 ms durations; their completion would generally take approximately an hour of computational calculation. The hourglass energy of the model remained under five percent of the total energy.

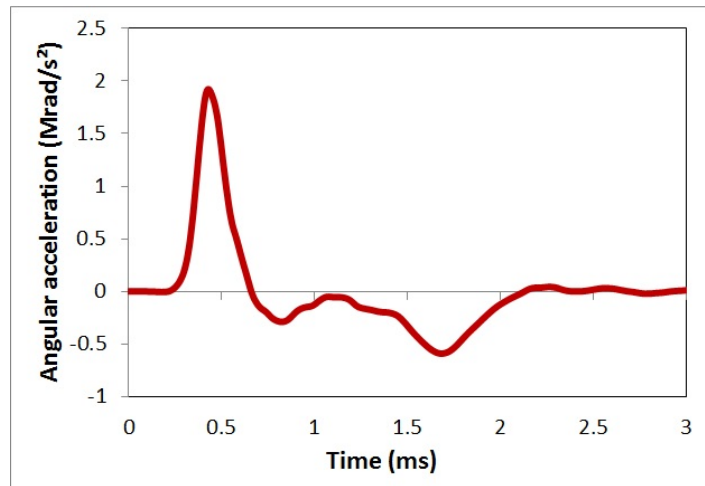


Figure 2. Representative acceleration time-history applied to the FEM. This particular acceleration corresponds to a severe case (maximum amplitude close to 2 Mrad/s²).

The main results acquired from the numerical simulations consisted of mechanical responses at tissue levels. Though the global distributions of mechanical responses were analyzed, the stress analysis output was extracted for three anatomical components of interest in the brain model: the cingulate cortex, the hippocampus and the superior colliculous (Figure 3). The cingulate cortex was chosen based on direct histological findings of the experimental setup. The hippocampus and superior colliculous were chosen because they are the components in the current subdivisions of the FEM that would correspond to the vicinity of the corpus callosum. Strain and stress data in particular were observed and evaluated in these regions, more specifically maximum principal strains and Von Mises stresses. For each parameter, after the complete anatomical distributions were analyzed, time history data were obtained for each element in the model. Consequently, the mean values of the parameters were evaluated as functions of time for each component. Thus, anatomical distributions and peak mean values of the studied parameters were used to try and quantify the consequences of the rotational acceleration loading. Furthermore, the mechanical results of the study were eventually compared to histological scores from the experimental setup so that potential mechanical thresholds could be proposed.

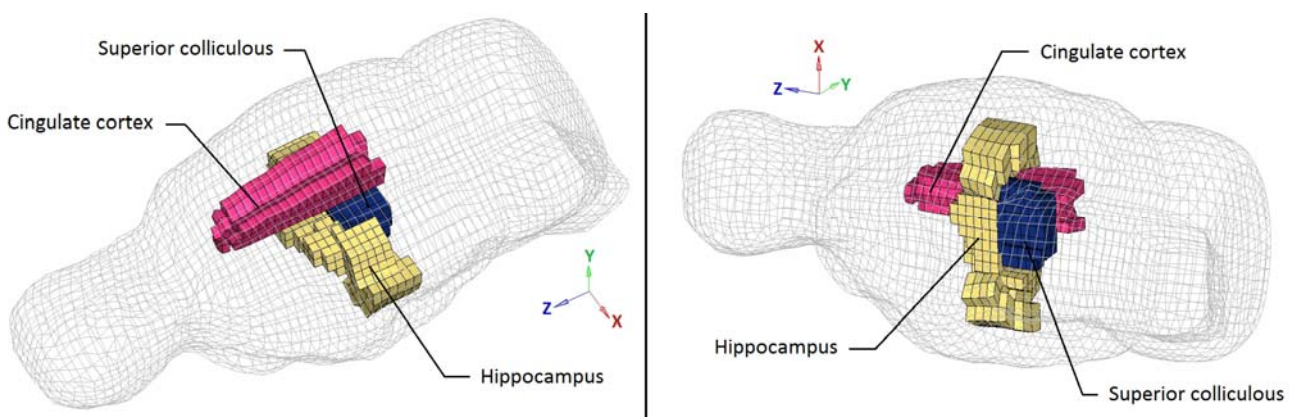


Figure 3. The three components which received special investigation in the study (cingulate cortex, hippocampus and superior colliculous) are presented from two different points of view.

III. RESULTS

General Results

The distributions of Von Mises stresses and first principal strains, and their temporal variations, were observed for each of the 47 simulations. Though the values of the mechanical responses varied depending on the simulation and the original associated loading, all simulations provided similar results in terms of spatial

distributions.

Both stresses and strains reached maximal values in the cingulate cortex component in the upper cerebrum. At the same time, a secondary core of high mechanical responses was observed in the more central parts of the brain model in the vicinities of the hippocampus and superior colliculus.

Figure 4 presents the distributions of both first principal strains and Von Mises stresses in the mid-sagittal plane after 1.7 ms of computation for a 2.09 Mrad/s² loading, which was the instant of maximal mechanical response for this particular simulation. The reported distributions in Figure 4 correspond to the general patterns for the instants of maximal mechanical responses in all simulations.

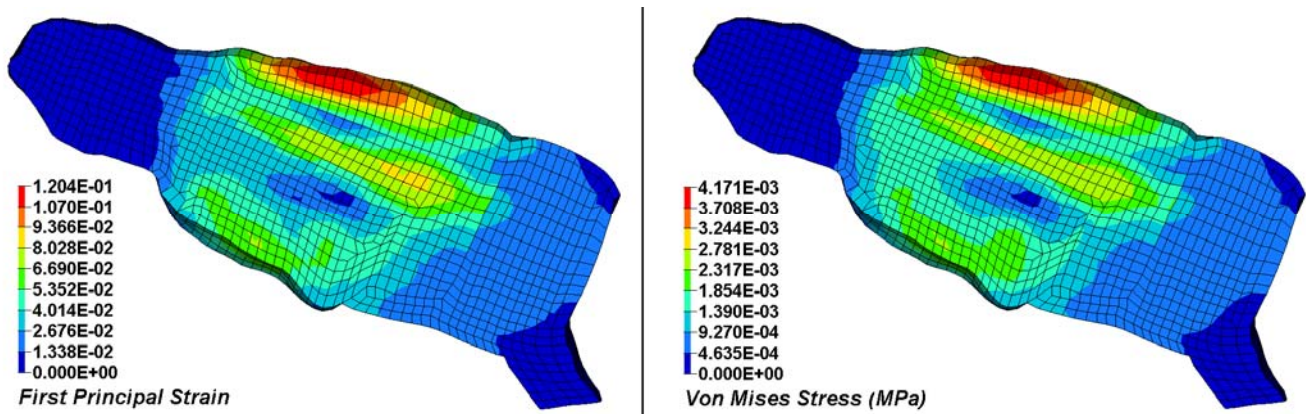


Figure 4. First principal strains (left) and Von Mises stresses (right) observed in the mid-sagittal plane at the instant when maximal values were reached for a 2.09 Mrad/s² angular acceleration loading.

Relations between Imposed Acceleration Amplitudes and Mechanical Responses

The variations of the Von Mises stresses and first principal strains were analyzed as potential functions of the amplitude of the imposed angular acceleration loadings. For each of the three regions of interest, the general positions of maximal responses were extracted from the analyzed distributions. As a consequence, the maximal Von Mises stresses and maximal first principal strains were estimated as mean peak values based upon 20 elements for the cingulate cortex, 14 elements for the hippocampus and 16 elements for the cingulate cortex. Thus, the occurrence of isolated elements, presenting maximal but not meaningful values, was avoided.

Figure 5 presents the reported variations. For all three regions, both the maximal stresses and maximal strains appeared to increase almost linearly with the applied angular acceleration loadings amplitudes.

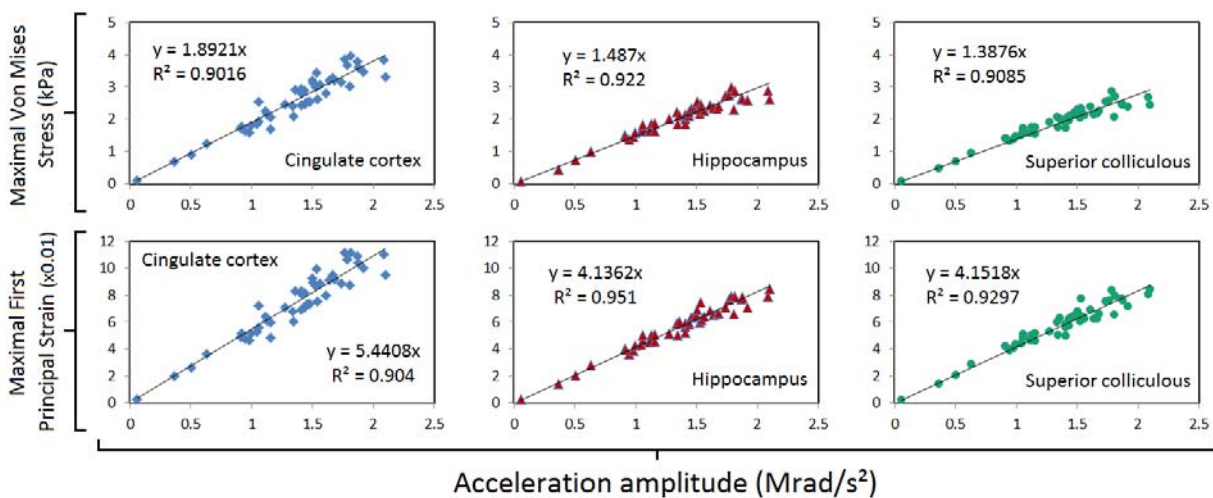


Figure 5. Imposed acceleration amplitudes compared with resulting maximal Von Mises stresses (upper line) and maximal first principal strains (lower line) in the cingulate cortex (left column), the hippocampus (middle column) and the superior colliculus (right column).

***β*-APP Scores vs Von Mises Stresses**

The maximum Von Mises stresses responses in the cingulate cortex, hippocampus and superior colliculus were extracted for all 47 simulations. Among those simulations, 27 had corresponding available β -APP scores. As such, β -APP scores and Von Mises stresses were analyzed together for the three regions of interest in those 27 cases as shown in Figure 6. For each of the three regions, higher β -APP scores were associated with loadings which had also caused higher maximal Von Mises stresses.

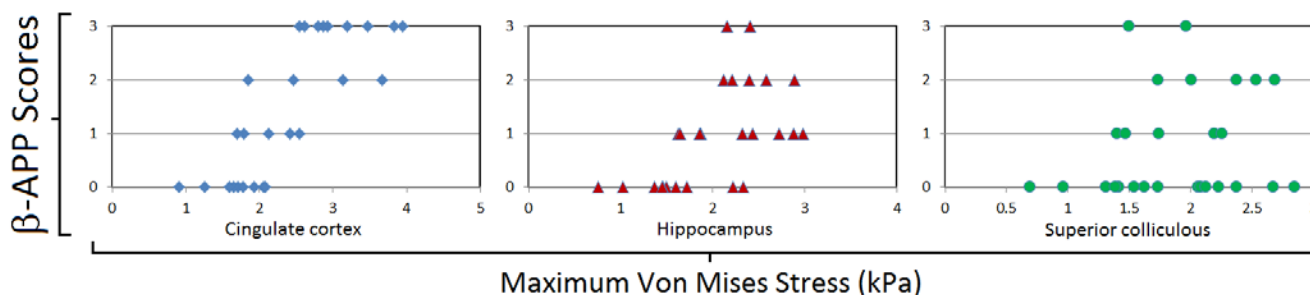


Figure 6. Relationship between β -APP scores and Von Mises stresses in the regions of interest.

β -APP Scores vs First Principal Strains

The maximum first principal strain responses were analyzed in the cingulate cortex, hippocampus and superior colliculus for all 47 simulations. As with Von Mises stresses, first principal strains were compared in all regions of interest with β -APP scores for the 27 cases which had received said scores as shown in Figure 7. For each of the three regions, the cases which displayed higher maximal first principal strains were also cases which had received higher β -APP scores.

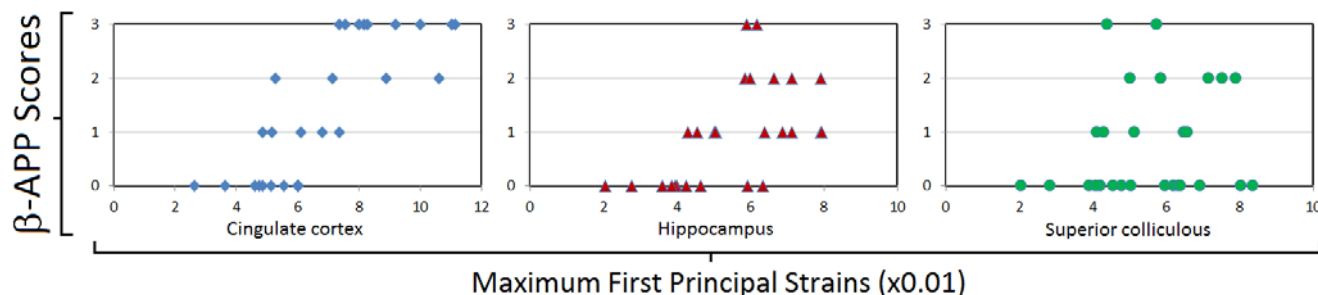


Figure 7. Relationship between β -APP scores and first principal strains in the regions of interest.

COX-2 Scores vs Von Mises Stresses

Similar to the comparison between maximal Von Mises stresses and β -APP scores, another analysis was carried out to examine the possible correlations between the Von Mises stresses and COX-2 scores. Among the 47 simulated cases, 22 had associated COX-2 histological results. Figure 8 presents the results of the analysis. Based on those 22 cases, and for each of the three regions, it appeared that the higher COX-2 scores were obtained with loadings which were responsible for the higher maximal Von Mises stresses.

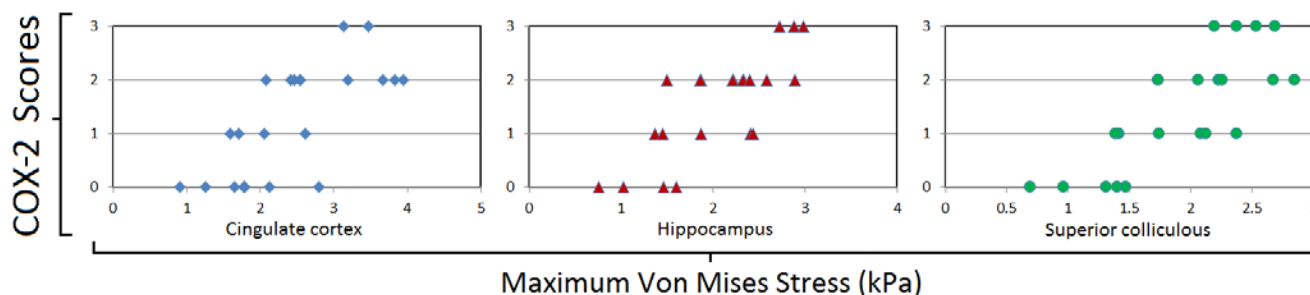


Figure 8. Comparison between COX-2 scores and Von Mises stresses in the regions of interest.

COX-2 Scores vs First Principal Strains

In addition to the Von Mises stresses, COX-2 scores were also compared with the maximal first principal

strains in the three regions of interest. The results which are presented by Figure 9 were quite similar to the stress results in that parallel increases were observed between the COX-2 scores and the maximal first principal strains.

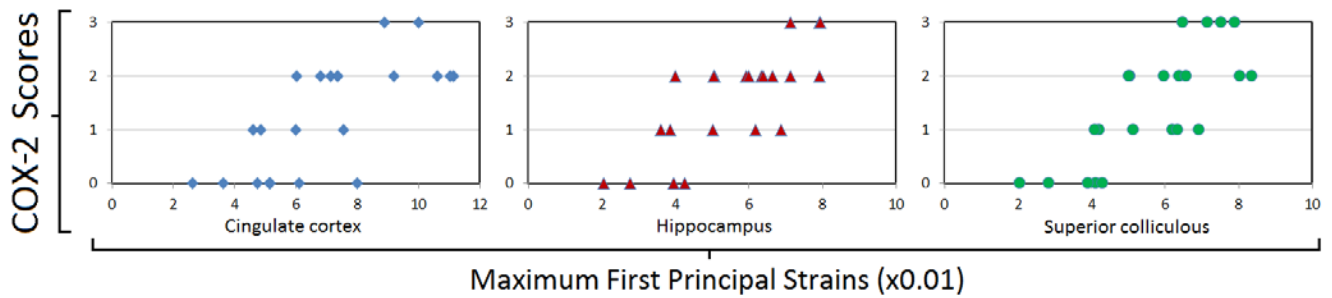


Figure 9. Comparison between COX-2 scores and first principal strains in the regions of interest

First Estimation of Von Mises Stresses and First Principal Strains Thresholds

Figures 6 to 9 suggest that β -APP and COX-2 scores are increasing after a stress or strain threshold has been reached. Thus, results were analyzed a second time by plotting stresses and strains as functions of the histological scores. Then, linear regressions were made and their parameters are shown in Tables 4 and 5. In particular, thresholds were estimated from the obtained linear equations as the strain or stress values which were given by these equations for a score of 0. Those thresholds are to be seen as the values of sustained mechanical responses for which the histological scores are not null anymore.

TABLE 4: RESULTS OF LINEAR REGRESSION ANALYSIS CORRELATING STRESS AND STRAIN DATA WITH β -APP SCORES

Parameter	Details	Anatomical region		
		Cingular cortex	Hippocampus	Superior colliculous
Strain	Slope [%]	1.4167	0.9483	0.2751
	R ²	0.6432	0.3202	0.0309
	Threshold [%]	4.7914	4.5401	5.3358
Stress	Slope [kPa]	0.4994	0.3451	0.0952
	R ²	0.6479	0.3196	0.0323
	Threshold [kPa]	1.6628	1.6828	1.8121

TABLE 5: RESULTS OF LINEAR REGRESSION ANALYSIS CORRELATING STRESS AND STRAIN DATA WITH COX-2 SCORES

Parameter	Details	Anatomical region		
		Cingular cortex	Hippocampus	Superior colliculous
Strain	Slope [%]	1.6577	1.381	1.2674
	R ²	0.5081	0.6067	0.6067
	Threshold [%]	4.8868	3.4101	3.8157
Stress	Slope [kPa]	0.5803	0.5091	0.4292
	R ²	0.5054	0.6203	0.6089
	Threshold [kPa]	1.6979	1.2648	1.298

Tables 4 and 5 presented results for the three regions of interest. To propose thresholds for the general brain, weighted means have been calculated. The thresholds of the three regions were taken into account, while the R² coefficients of the linear regressions served as weights for the estimation of the mean. Table 6 regroupes the global proposed thresholds.

TABLE 6: PROPOSED THRESHOLDS FOR VON MISES STRESS AND FIRST PRINCIPAL STRAIN

	Stress threshold [kPa]	Strain threshold [%]
β -APP analysis	1.674	4.727
COX-2 analysis	1.403	3.989

IV. DISCUSSION

Concerning the Choice of the Rodent Model

In order to complement anatomical and histological findings from a controlled experimental setup [17-20], the three-dimensional finite element model of the rat brain was used for the examination of the region-specific intrinsic mechanical variables. While there are obvious fundamental differences in the brains between a rodent one and a human one, such as composition of gray and white matter, or different sizes and shapes, at the tissue or cellular level cerebral structures are more comparable [13]. As such, the present study should be considered a first step toward an improved understanding of the angular loading-caused intrinsic biomechanics of mild TBI. Moreover, it should be stressed that the experimental animal model used in the present study has long been used by brain injury researchers. For these reasons, information on lesions and thresholds obtained from the rat model can prove to be relevant for the study of injury mechanisms. Still, additional studies are needed to fully understand the mechanics of mild TBI and to translate or confirm the knowledge acquired from the rodent brain to the human brain.

Rationale for the Evaluation of Stress and Strain Variables

The Introduction pointed out that finite element models of the rat brain have been developed to simulate a varied array of loadings: dynamic cortical deformations [23] to study injuries to the blood-brain barrier; controlled cortical impacts [24-25] to complement experimental indentation data [26]; inertial loading to examine strain-time based parameters for hippocampal damage [22]. However, the present model is the first complete three-dimensional TBI-specific model to correlate stress- and strain-related data in different regions of the brain with histological evidence of graded TBI caused by angular acceleration collisions.

The present work included the Von Mises stress as a variable of particular interest, since previous studies correlated the peak Von Mises stress with neurological outcomes and cerebral injuries in animal and human models [31, 40-42]. Similarly, strains have been proposed as indicators of levels of cerebral injuries [26, 30, 43-44], resulting in their inclusion as variables in the present study. Furthermore, the amplitude of angular acceleration loading has been shown in the experimental setup, which was numerically simulated by the present work, to be related to the varying severity of TBI; it was proposed that a 1.1 Mrad/s² loading was the limit after which TBI were likely to occur [17]. The current work showed that the Von Mises stresses and first principal strains increased with the amplitude of the acceleration loading and therefore could be used as mechanical thresholds for the severity of TBI.

The three regions of interest studied were chosen because of the histological evidence in the experimental setup. Simulations revealed the cingulate cortex as being the part of the brain which experienced the highest stresses and strains. However, it should be noted that the shape of the skull component is slightly protruding inward just above the upper central surface of the brain in the mid-sagittal plane and thus above the cingulate cortex. This could have resulted in a slight increase in the mechanical responses in the cingulate cortex component. Also, stresses and strains displayed the hippocampus and superior colliculous vicinities as secondary regions of high mechanical responses, correlating with the histological evidence. The importance of those internal regions is further supported by the centripetal theory that clinical concussion, resulting from applying rotational accelerations, was attributed to stresses/strains initiating from the surface (cortex, mild cases) and progressing towards the diencephalic and mesencephalic cores (more severe cases) [6, 45].

Comparison with Literature

As mentioned previously, other finite element modeling studies have included magnitudes of strains as

thresholds for cerebral injuries. In 2006, based on controlled cortical impact loading applied to a rat finite element model, Mao et al. reported that a strain level of 0.30 represents contusive brain injury [26]. In 2006, Cater et al. [46] found, from an in-vitro model of TBI based on hippocampal slice cultures, that a 0.20 strain would result in significant percentages of cell death, and that these percentages depended on the strain magnitude and also on the region of the hippocampus. In 2007, a continuation of the previous study showed that tolerance was region-based, with cortex having a lower strain threshold than hippocampus [47]. In 2007, Kleiven et al. used the maximum principal strain as a metric for predicting concussion: 50% risk of concussion was estimated at a strain level of 0.21 in the corpus callosum and the same magnitude was also applicable for the gray matter [44]. In 2008, using the Strasbourg University Finite Element Head Model, the first principal strain was proposed as a criterion to assess diffuse axonal injury: a strain level of 0.31 corresponded to 50% injury risk [30]. Recently, a FEM of the monkey head also found an association between a 50% risk of concussion and a sustained strain of 0.21 [48]. Strains have also been explored in in-vivo conditions. In 2008 Sabet et al. observed deformations in human volunteers under mild angular acceleration loading using tagged magnetic resonance images and reported that large portions of the brain sustain strains exceeding 0.02 [49]. Most of the aforementioned studies dealt with conditions different from the present study: some had direct contact impact, creating high strains near the contact interface [26], while other studies were based on experimental or numerical models of the human brain [30, 49] or the non-human primate brain [48]. Differences in the strain level may be due to these variations. Furthermore, the aforementioned studies proposed strains thresholds designed to elaborate on a percentage of risk of sustaining injuries. The current study proposes thresholds corresponding to the early occurrence of TBI, thus possibly resulting in lower strain values. Indeed, if the most severe cases only are considered in our study, then strain values are closer to 0.1 and thus more similar to the aforementioned values. Also, the results from this study were compared to available histological evidence and the brain was considered homogeneous. As a consequence, developing precise thresholds for the whole brain is not possible; thresholds can only be evaluated in selected regions.

In the current three-dimensional model, the rat head was subjected to inertial loadings without direct contact. This necessitated the application of greater levels of loadings/rotational acceleration to achieve outcomes similar to those observed in the human [6, 50-51]. It also has consequences on the direct response of the finite element modeling of the brain. Using a human brain finite element model, it has been shown that the size of the brain model affects the biomechanical outputs such as internal stresses [52].

The mechanical responses are also influenced by the chosen material modeling. Through parametric studies, it has been shown that these responses, Von Mises stresses in particular, will have varying maximal peak values depending on different material parameters, though the global patterns of distribution will be largely unaffected by the changes in these parameters [53]. As such, it is important to remember that the thresholds are strongly related to the model and should be considered only in light of the FEM precise setup. For example, if the short term shear modulus is doubled, the Von Mises stresses will also be increased twofold [53]. Strains, on the other hand, will decrease with the short-term shear modulus, though not significantly over a reasonable range for this modulus. Furthermore, if a more detailed characterization of brain matter were to be implemented, it might modify local distributions of mechanical responses at boundaries between anatomical components, though maybe not the global distribution. Still, differentiating white matter from grey matter would require a change in white matter material properties, and consequently would change Von Mises stress and first principal strain in this white matter, meaning a possible modification of the thresholds. In summary, the thresholds remain model-bound and the Von Mises stress threshold in particular is very dependent on assigned material properties.

Also of interest are the relative magnitudes of strains and stresses in the three anatomical regions of the brain that were studied. The highest values were reported in the cingulate cortex followed by the hippocampus and the superior colliculus. This would be in accordance with the centripetal force theory [45] as the cingulate cortex is situated along the upper surface of the brain while the other two regions are more central and closer to the centre of rotation. This observation also addresses some aspects of the FE model. It is considered homogeneous and made only of gray matter. However, a differentiation between gray and white matter properties could affect the results of the model. By using available subcomponents of the cerebrum and material data, an anatomically-related definition of material properties and more accurate region-specific mechanical responses could be developed. These are considered future research directions.

V. CONCLUSIONS

A finite element model of the rat brain and skull was used to simulate head sagittal angular accelerations based on data from animal experiments. This combined approach of numerical modeling and animal experiments allowed for the investigation of region-dependent mechanical responses of the anatomical components of the brain. These responses were stresses and strains, and were analyzed in relation to histological scores that quantified DBI in the experimental setup. The experimental acceleration pulses covered a variety of grades of severity as evidenced by the histological results. First principal strains and Von Mises stresses matched variations of peak angular accelerations in the regions of interest for the numerical FEM. They were also correlated with the histological scores which lead to a first estimation of potential thresholds for stresses and strains to correspond to the occurrence of DBI. Those thresholds, used in conjunction with the rat FEM, can be used in future new simulations of collisions to gain further knowledge and insight about the mechanics of TBI.

VI. REFERENCES

- [1] Tagliaferri F, Compagnone C, Korsic M, Servadei F and Kraus J, A systematic review of brain injury epidemiology in Europe, *Acta Neurochir (Wein)*, 148:255-268, 2006.
- [2] Centers for Disease Control and Prevention: <http://www.cdc.gov/traumaticbraininjury/severe.html> [accessed on March 21st 2013].
- [3] Gennarelli TA and Meaney DF, Mechanisms of primary head injury, *Neurosurgery*, eds. R Wilkins and S Rengachary, *McGraw Hill*, New York, pp. 2611-2621, 1996.
- [4] Lissner HR, Lebow M and Evans FG, Experimental studies on the relation between acceleration and intracranial pressure changes in man, *Surg Gynecol Obstet*, 111:329-338, 1960.
- [5] Yoganandan N, Pintar FA, Larson SJ and Sances A Jr, eds. *Frontiers in Head and Neck Trauma: Clinical and Biomechanical*, *IOS Press*, The Netherlands, 1998.
- [6] Holbourn AHS, The mechanics of brain injuries, *British Medical Bulletin*, 3:144-149, 1945.
- [7] Gennarelli TA, Thibault LE, Adams JH, Graham DI, Thompson CJ and Marcincin RP, Diffuse axonal injury and traumatic coma in the primate, *Annals of Neurology*, 12(6):564-574, 1982.
- [8] Zhang J, Yoganandan N, Pintar FA and Gennarelli TA, Brain strains in vehicle impact tests, *Annu Proc Assoc Adv Automot Med*, 50:1-12, 2006.
- [9] King A, Yang KH, Zhang L and Hardy WN, Is head injury caused by linear or angular acceleration?, *Proceedings of the 2003 IRCOBI Conference*, Lisbon, Portugal, pp. 1-12, 2003.
- [10] *Abbreviated Injury Scale*, *American Association for Automotive Medicine*, Arlington Heights, IL, 1990.
- [11] Dixon CE, Clifton GL, Lighthall JW, Yaghmai AA and Hayes RL, A controlled cortical impact model of traumatic brain injury in the rat, *J Neurosci Methods*, 39(3):253-262, 1991.
- [12] Lighthall JW, Controlled cortical impact: a new experimental brain injury model, *J Neurotrauma*, 5(1):1-15, 1988.
- [13] Shreiber DI, Bain AC, Ross DT, Smith DH, Gennarelli TA, McIntosh TK and Meaney DF, Experimental investigation of cerebral contusion: histopathological and immunohistochemical evaluation of dynamic cortical deformation, *J Neuropathol Exp Neurol*, 58(2):153-164, 1999.
- [14] Dixon CE, Lyeth BG, Povlishock JT, Findling RL, Hamm RJ, Marmarou A, Young HF and Hayes RL, A fluid percussion model of experimental brain injury in the rat, *Journal of Neurosurgery*, 67(1):110-119, 1987.
- [15] Lindgren S and Rinder L, Production and distribution of intracranial and intraspinal pressure changes at sudden extradural fluid volume input in rabbits, *Acta Physiol Scand*, 76(3):340-351, 1969.
- [16] Marmarou A, Foda MA, van den Brink W, Campbell J, Kita H and Demetriadou K, A new model of diffuse brain injury in rats. Part I: Pathophysiology and biomechanics, *Journal of Neurosurgery*, 80(2):291-300, 1994.
- [17] Davidsson J, Risling M and Angeria M, A new model and injury threshold for sagittal plane rotational induced diffuse axonal injuries in the brain, *Proceedings of the 2009 IRCOBI Conference*, York, UK, pp. 73-80, 2009.
- [18] Risling M, Plantman S, Angeria M, Rostami E, Bellander BM, Kirkegaard M, Arborelius U and Davidsson J, Mechanisms of blast induced brain injuries, experimental studies in rats, *NeuroImage*, 54:89-97, 2010.

- [19] Davidsson J and Risling M, A new model to produce sagittal plane rotational induced diffuse axonal injuries, *Frontiers in Neurology*, 2(41), 2011.
- [20] Rostami E, Davidsson J, Ng KC, Lu J, Gyorgy A, Wingo D, Walker J, Plantman S, Bellander BM, Agoston DV and Risling M, A model for mild traumatic brain injury that induces limited transient memory impairment and increased levels of axon related serum biomarkers, *Frontiers in Neurology*, 3(115), 2012.
- [21] Fijalkowski RJ, Stemper BD, Pintar FA, Yoganandan N, Crowe MJ and Gennarelli TA, New rat model for diffuse brain injury using coronal plane angular acceleration, *J Neurotrauma*, 24(8):1387-1398, 2007.
- [22] Fijalkowski RJ, Yoganandan N, Zhang J and Pintar FA, A finite element model of region-specific response for mild diffuse brain injury, *Stapp Car Crash J*, 53:193-213, 2009.
- [23] Shreiber DI, Bain AC and Meaney DF, In vivo thresholds for mechanical injury to the blood-brain barrier, *41st Stapp Car Crash Conf*, pp. 277-292, 1997.
- [24] Gefen A, Gefen N, Zhu Q, Raghupathi R and Margulies SS, Age-dependent changes in material properties of the brain and braincase of the rat, *J Neurotrauma*, 20(11):1163-1177, 2003.
- [25] Levchakov A, Linder-Ganz E, Raghupathi R, Margulies SS and Gefen A, Computational studies of strain exposures in neonate and mature rat brains during closed head impact, *J Neurotrauma*, 23(10):1570-1580, 2006.
- [26] Mao H, Zhang L, Yang KH and King AI, Application of a finite element model of the brain to study traumatic brain injury mechanisms in the rat, *Stapp Car Crash J*, 50:583-600, 2006.
- [27] Zhu F, Mao H, Dal Cengio Leonardi A, Wagner C, Chou C, Jin X, Bir C, Vandevord P, Yang KH and King AI, Development of a finite element model of the rat head subjected to air shock loading, *Stapp Car Crash J*, 54:211-225, 2010.
- [28] Cernak I, O'Connor C and Vink R, Inhibition of cyclooxygenase 2 by nimesulide improves cognitive outcome more than motor outcome following diffuse traumatic brain injury in rats, *Exp Brain Res*, 147:193-199, 2002.
- [29] Hickey RW, Adelson PD, Johnnides MJ, Davis DS, Yu Z, Rose ME, Chang YF and Graham SH, Cyclooxygenase-2 activity following traumatic brain injury in the developing rat, *Pediatr Res*, 62(3):271-276, 2007.
- [30] Deck C and Willinger R, Improved head injury criteria based on head FE model, *Int J Crashworthiness*, 13(6):667-678, 2008.
- [31] Baumgartner D and Willinger R, Human head tolerance limits to specific injury mechanisms inferred from real world accident numerical reconstruction, *Revue Européenne des Eléments Finis*, 14(4-5):421-444, 2004.
- [32] Mao H and Wagner C, Material properties of adult rat skull, *Journal of Mechanics in Medicine and Biology*, 11(5):1199-1212, 2011.
- [33] Guan F, Han X, Mao H, Wagner C, Yeni YN and Yang KH, Application of optimization methodology and specimen-specific finite elements models for investigating material properties of rat skull, *Annals of Biomedical Engineering*, 39(1):85-95, 2011.
- [34] Vappou J, Breton E, Choquet P, Willinger R and Constantinesco A, Assessment of in vivo and post-mortem mechanical behavior of brain tissue using magnetic resonance elastography, *Journal of Biomechanics*, 41:2954-2959, 2008.
- [35] Elkin BS, Azeloglu EU, Costa KD and Morrison III B, Mechanical heterogeneity of the rat hippocampus measured by AFM indentation, *J Neurotrauma*, 24(5):812-822, 2007.
- [36] Elkin BS, Ilankovan A and Morrison III B, A detailed viscoelastic characterization of the p17 and adult rat brain, *J Neurotrauma*, 28(11):2235-2244, 2011.
- [37] Finan JD, Elkin BS, Pearson EM, Kalbian IL and Morrison III B, Viscoelastic properties of the rat brain in the sagittal plane: Effects of anatomical structure and age, *Ann Biomed Eng*, 40:70-78, 2012.
- [38] Finan JD, Pearson EM and Morrison III B, Viscoelastic properties of the rat brain in the horizontal plane, *Proceedings of the 2012 IRCOBI Conference*, Dublin, Ireland, 2012.
- [39] Lamy M, Baumgartner D, Willinger R and Yoganandan N, Mild traumatic brain injury in the rat: three-dimensional finite-element model using experimental data, *Proceedings of the 2011 IRCOBI Conference*, Krakow, Poland, pp. 23-35, 2011.
- [40] Marjoux D, Baumgartner D, Deck C and Willinger R, Head injury prediction capability of the HIC, HIP, SIMon and ULP criteria, *Accid Anal Prev*, 40(3):1135-1148, 2008.
- [41] Anderson RW, Brown CJ, Blumbergs PC, McLean AJ and Jones NR, Impact mechanics and axonal injury in a sheep model, *J Neurotrauma*, 20(10):961-974, 2003.

- [42] Anderson RW, Brown CJ, Blumbergs PC, Scott G, Finnie J, Jones NR and McLean AJ, Mechanisms of axonal injury: an experimental and numerical study of a sheep model of head impact, *Proceedings of the 1999 IRCOBI Conference*, Sitges, Spain, pp. 107-120, 1999.
- [43] Bain AC and Meaney DF, Tissue-level thresholds for axonal damage in an experimental model of central nervous system white matter injury, *J Biomech Eng*, 122 (6):615-622, 2000.
- [44] Kleiven S, Predictors for traumatic brain injuries evaluated through accident reconstructions, *Stapp Car Crash J*, 51:81-114, 2007.
- [45] Ommaya AK, and Gennarelli TA, Cerebral concussion and traumatic unconsciousness. Correlation of experimental and clinical observations of blunt head injuries, *Brain*, 97(4):633-654, 1974.
- [46] Cater HL, Sundstrom LE and Morrison III B, Temporal development of hippocampal cell death is dependent on tissue strain but not strain rate, *J Biomech*, 39(15):2810-2818, 2006.
- [47] Elkin BS and Morrison III B, Region-specific tolerance criteria for the living brain, *Stapp Car Crash J*, 51:127-138, 2007.
- [48] Antona-Makoshi J, Davidsson J, Ejima S and Ono K, Reanalysis of monkey head concussion experiment data using a novel monkey finite element model to develop brain tissue injury reference values, *Proceedings of the 2012 IRCOBI Conference*, Dublin, Ireland, 2012.
- [49] Sabet AA, Christoforou E, Zatlin B, Genin GM and Bayly PV, Deformation of the human brain induced by mild angular head acceleration, *J Biomech*, 41(2):307-315, 2008.
- [50] Margulies SS and Gennarelli TA, A study of scaling and head injury criteria using physical model experiments, *Proceedings of the 1985 IRCOBI Conference*, Goteborg, Sweden, pp. 223-234, 1985.
- [51] Ommaya AK, Yarnell P and Hirsch AE, Scaling of experimental data on cerebral concussion in subhuman primates to concussion threshold for man, *11th Stapp Car Crash Conf*, pp. 73-80, 1967.
- [52] Kleiven S and von Holst H, Consequences of head size following trauma to the human head, *J Biomech*, 35(2):153-160, 2002.
- [53] Baumgartner D, Lamy M, Willinger R, Choquet P, Goetz C, Constantinesco A, and Davidsson J, Finite element analysis of traumatic brain injuries mechanisms in the rat, *Proceedings of the 2009 IRCOBI Conference*, York, UK, pp. 97-108, 2009.